
SKewed LAPLACE SPECTRAL MIXTURE KERNELS FOR LONG-TERM FORECASTING IN GAUSSIAN PROCESS

A PREPRINT

Kai Chen

Institute for Computing and Information Sciences, Radboud University
kyoungchen@gmail.com

Twan van Laarhoven

Institute for Computing and Information Sciences, Radboud University
twanvl@gmail.com

Elena Marchiori

Institute for Computing and Information Sciences, Radboud University
elenam@cs.ru.nl

May 1, 2022

ABSTRACT

Long-term forecasting involves predicting a horizon that is far ahead of the last observation. It is a problem of highly practical relevance, for instance for companies in order to decide upon expensive long-term investments. Despite recent progress and success of Gaussian Processes (GPs) based on Spectral Mixture kernels, long-term forecasting remains a challenging problem for these kernels because they decay exponentially at large horizons. This is mainly due their use of a mixture of Gaussians to model spectral densities. The challenges underlying long-term forecasting become evident by investigating the distribution of the Fourier coefficients of (the training part of) the signal, which is non-smooth, heavy-tailed, sparse and skewed. Notably the heavy tail and skewness characteristics of such distribution in spectral domain allow to capture long range covariance of the signal in the time domain. Motivated by these observations, we propose to model spectral densities using a Skewed Laplace Spectral Mixture (SLSM) due to the skewness of its peaks, sparsity, non-smoothness, and heavy tail characteristics. By applying the inverse Fourier Transform to this spectral density we obtain a new GP kernel for long-term forecasting. Results of extensive experiments, including a multivariate time series, show the beneficial effect of the proposed SLSM kernel for long-term extrapolation and robustness to the choice of the number of mixture components.

Keywords Skewed Laplace Distribution, Empirical Spectral Densities, Long Tail Distributions, Spectral Mixture, Gaussian Process, Long Term Forecasting

1 Introduction

Gaussian Processes (GPs) are an elegant Bayesian approach to modeling an unknown function. They provide regression models where a posterior distribution over the unknown function is maintained as evidence is accumulated. This allows GPs to learn involved functions when a large amount of evidence is available, and makes them robust against overfitting in the presence of little evidence [1, 2]. A GP can model a large class of phenomena through the choice of its kernel, which characterizes one's assumption about the autocovariance of the unknown function. Therefore, the choice of the kernel is a core step when designing a GP, since the posterior distribution can significantly vary for different kernels.

Important advances in the design of kernel functions for GPs have been achieved in recent years. In particular, kernels based on exponential distributions [3, 4, 5, 6, 7], notably the flexible Spectral Mixture (SM) kernels, have been successfully applied to many real-life extrapolation tasks. However, it remains challenging for SM kernels to perform long-term forecasting because they decay exponentially at large distances.

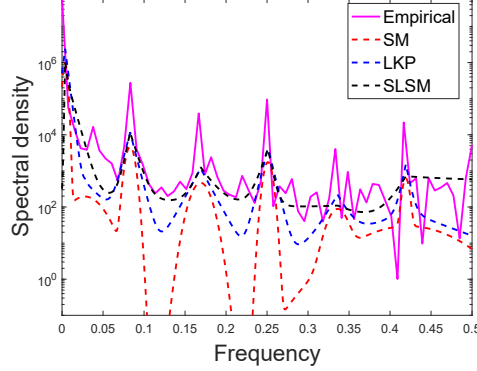


Figure 1: Empirical spectral density (magenta solid line) of the rail passenger miles (training) dataset described in Section 6.1. We have fitted an SM kernel (red dashed line), LKP kernel (blue dashed), and SLSM kernel (black dashed) on this empirical spectral density (using least squares). Skewness of the peaks in the empirical density can be observed for the first, third, and fourth peak, which are right tailed. SM and LKP cannot capture this one side heavy tail characteristics of the spectral density, while SLSM can. As a result it has a better fit. Note that even if differences between the kernels looks negligible in the figure, an exponential scale is used, so such differences are very significant.

The challenges underlying long-term forecasting become evident when we analyze the distribution of the Fourier coefficients of the signal, which is shown in Figure 1 for the (training part of the) Rail Passenger Miles dataset (described in Section 6.1). The Fourier coefficients distribution appears to be non-smooth, heavy-tailed, sparse and have skewed peaks. Notably the heavy tail and the skewness of peaks of the empirical spectral density correspond to long range covariance in the time domain. Figure 1 shows SLSM provides a better fit of the empirical spectral density than the Gaussian Spectral Mixture (SM) and the Lévy kernel Process (LKP), current state of the art spectral kernels.

The inverse Fourier transform of an SM spectral density is an exponential function, so in the time domain we have an exponential decay of covariance. When we use LKP to fit the empirical spectral density and apply the inverse Fourier transform we get a Cauchy function, which has a much slower decay than that of the exponential function. Using SLSM we extend the tails of the Laplace distribution (by means of the γ term in Equation (7)), which in the time domain yields a further reduction of the decay rate of the covariance. This is illustrated in Figure 2, middle and bottom right plots, which shows longer range covariance of SLSM.

Motivated by these observations, as well as by previous work on modeling the asymmetric tails of discrete Fourier transform coefficients distributions [8, 9, 10], we investigate the use of skewed Laplace mixture to model the spectral density, that is, the Fourier transform (FT) of a kernel. We then use the inverse Fourier transform to construct a kernel for GP, which we call Skewed Laplace Spectral Mixture (SLSM) kernel. Our contributions can be summarized as follows:

- the difficulty of long trend forecasting with GP's is linked to long range characteristics of covariance between random vectors, which are determined by properties of the spectral density, namely sparseness, skewed peaks, long tails, and non-smoothness;
- a new GP kernel for long-term forecasting is introduced, which includes a skewness term that allows to model a different tails for the two sides of each spectral peak.
- a comparative analysis of the SLSM and other spectral kernels, in particular a connection between the SLSM kernel and the popular Rational Quadratic kernel;
- extensive long-term forecasting experiments with various time series data, including a multivariate and a large dataset. Results of experiments indicate state of the art performance of GP's with the SLSM kernel and robustness to overfitting when considering hundreds of mixture components.

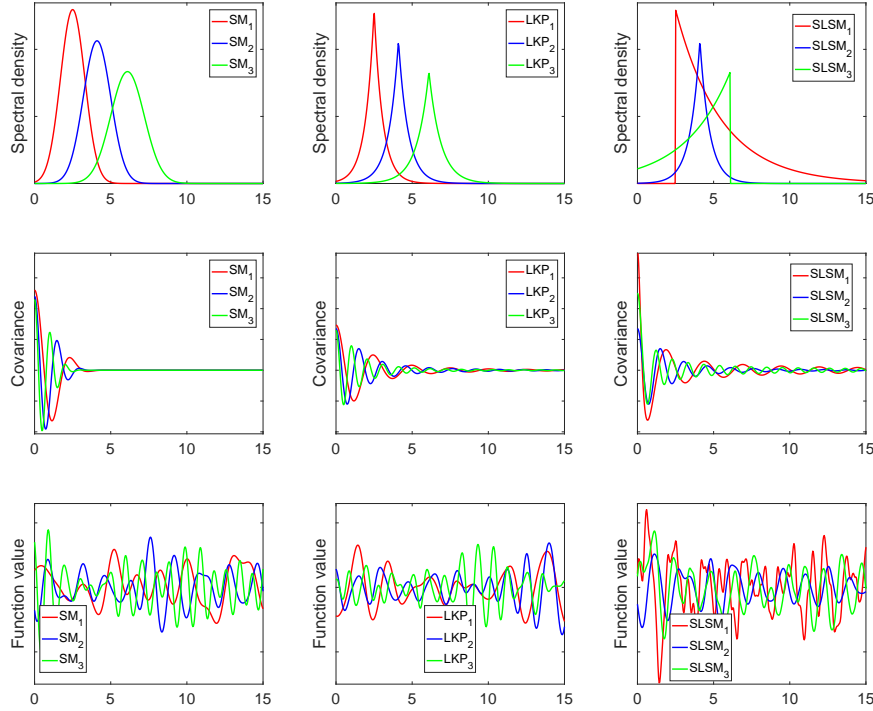


Figure 2: SM (left), LKP (middle), and SLSM (right) kernels with three different choices of amplitude, mean and variance. In the top figures we can see the different shapes of the spectral density, and the flexibility provided by the skewness parameter in the SLSM kernel. From the covariance functions, shown in the middle row, we see that SM only has a very short range covariance (range $\tau < 5$). LKP has longer range covariance (range $\tau \leq 15$) because of the heavier tails in the spectral density. The SLSM kernel has the longest covariance representation range ($\tau \gg 15$) due to skewness in the frequency domain. In the bottom row we show draws from Gaussian Processes with these kernels. The SLSM kernel results in a larger variance, which is more flexible and less smooth than SM and LKP, because of heavy tails at high frequency position in the frequency domain. Both positive and negative skewness (determined by γ) in SLSM can extend covariance range and therefore increase the variance in the sampled functions. A positive (skewness) value of γ contributes more to signal variance.

The rest of the paper is organized as follows. In the next section we summarize related works. Section 3 and 4 introduce GPs and the SM kernel. Then in Section 5 we introduce the SLSM kernel. Section 6 describes hyper-parameters initialization and experiments on real-world datasets. Concluding remarks and future work are given in Section 7.

2 Related Work

The popularity and success of SM kernels [3, 11] has stimulated related research and kernel extensions [11, 5, 12, 13, 7]: from the spectral mixture product kernel [11] modeling Cartesian structured datasets, to the non-stationary SM kernel modeling input-dependent GP's [6]. All these works consider a Gaussian as a base representation of the spectral density, which corresponds to an exponential function for the covariance in the time domain. Various works [8, 14, 9] showed the inadequacy of Gaussian mixture or its inverse for modeling spectral densities. The Laplace distribution has been successfully used for representing the non-smooth, sparse and heavy-tailed distribution of the DFT coefficients in order to perform speech recognition [8, 9], JPEG image compression [10] and image segmentation [14].

The Lévy kernel process (LKP) with sparsity-inducing prior over mixture components [7] was used for modeling the sharply peaked spectral density with a location-scale mixture of Laplace components, which is more sparse than the SM kernel, hence more robust to the choice of the number of mixture components. LKP can discover heavy-tailed patterns which are useful for long range extrapolation. However it is only available for one dimensional inputs and does not consider the skewness of the spectral density.

3 Gaussian Processes

A Gaussian process defines a distribution over functions, specified by its mean function $m(\mathbf{x})$ and covariance function $k(\mathbf{x}, \mathbf{x}')$ [2] for given input vector $\mathbf{x} \in \mathbb{R}^P$. Thus we can define a GP as $f(\mathbf{x}) \sim \mathcal{GP}(m(\mathbf{x}), k(\mathbf{x}, \mathbf{x}'))$. Without loss of generality we assume the mean of a GP to be zero. The covariance function is applied to construct a positive definite covariance matrix on the set X training points, called the kernel and denoted by $K = K(X, X)$. By placing a GP prior over functions through the choice of a kernel and parameter initialization, from the training data X we can predict the unknown function value \tilde{y}_* and its variance $\mathbb{V}[\tilde{y}_*]$ (that is, its uncertainty) for a test point \mathbf{x}_* using the following key predictive equations for GP regression [2]:

$$\tilde{y}_* = \mathbf{k}_*^\top (K + \sigma_n^2 I)^{-1} \mathbf{y} \quad (1)$$

$$\mathbb{V}[\tilde{y}_*] = k(\mathbf{x}_*, \mathbf{x}_*) - \mathbf{k}_*^\top (K + \sigma_n^2 I)^{-1} \mathbf{k}_* \quad (2)$$

where \mathbf{k}_*^\top is the covariances vector between \mathbf{x}_* and X , and \mathbf{y} are the observed values corresponding to X . Typically, kernels contain free hyper-parameters, denoted by Θ , which can be optimized by minimizing the Negative Log Marginal Likelihood (NLML) of the observed values $y = f(X)$:

$$\begin{aligned} \text{NLML} &= -\log p(\mathbf{y}|X, \Theta) \\ &\propto \underbrace{\frac{1}{2} \mathbf{y}^\top (K + \sigma_n^2 I)^{-1} \mathbf{y}}_{\text{model fit}} + \underbrace{\frac{1}{2} \log |K + \sigma_n^2 I|}_{\text{complexity penalty}} \end{aligned} \quad (3)$$

where σ_n^2 is the noise level and NLML is obtained through marginalization over the latent function [2]. This formulation follows directly from the fact that $\mathbf{y} \sim \mathcal{N}(0, K + \sigma_n^2 I)$. In this paper we consider only stationary kernels, which are invariant to translation of the inputs. These can be described as functions of $\tau = \mathbf{x} - \mathbf{x}'$, $k(\mathbf{x}, \mathbf{x}') = k(\mathbf{x} - \mathbf{x}')$.

4 Spectral Mixture kernels

Recently, a class of flexible stationary kernels for GPs, called Spectral Mixture (SM) kernels, has been introduced [4, 3]. A SM kernel, here denoted by k_{SM} , is derived through modeling its spectral density (the Fourier transform of a kernel) with a Gaussian mixture. Such modeling is possible because of Bochner's Theorem [15, 16], which states that the properties of a stationary kernel entirely depend on its spectral density: A complex-valued function k on \mathbb{R}^P is the covariance function of a weakly stationary mean square continuous complex-valued random process on \mathbb{R}^P if and only if it can be represented as

$$k(\tau) = \int_{\mathbb{R}^P} e^{2\pi j \mathbf{s}^\top \tau} \psi(d\mathbf{s}),$$

where ψ is a positive finite measure. j denotes the imaginary unit. If ψ has a density $\hat{k}(\mathbf{s})$, then \hat{k} is called the spectral density or power spectrum of k , and k and \hat{k} are Fourier duals: $k(\tau) = \int \hat{k}(\mathbf{s}) e^{2\pi j \mathbf{s}^\top \tau} d\mathbf{s}$ and $\hat{k}(\mathbf{s}) = \int k(\tau) e^{2\pi j \mathbf{s}^\top \tau} d\tau$. The SM kernel is defined as the inverse Fourier transform (that is, the Fourier dual) of a mixture of Q components in the frequency domain:

$$k_{\text{SM}}(\tau) = \mathcal{F}_{\mathbf{s} \rightarrow \tau}^{-1} \left[\sum_{i=1}^Q w_i \hat{k}_{\text{SM},i} \right] (\tau), \quad (4)$$

where $\mathcal{F}_{\mathbf{s} \rightarrow \tau}^{-1}$ denotes the inverse Fourier transform operator from the frequency to the time domain, and w_i is the weight of component $\hat{k}_{\text{SM},i}$. Each of the Q components in the frequency domain is $\hat{k}_{\text{SM},i}(\mathbf{s}) = [\varphi_{\text{SM},i}(\mathbf{s}) + \varphi_{\text{SM},i}(-\mathbf{s})]/2$, where $\varphi_{\text{SM},i}(\mathbf{s}) = \mathcal{N}(\mathbf{s}; \boldsymbol{\mu}_i, \Sigma_i)$ is a scale-location Gaussian with parameters $\boldsymbol{\mu}_i, \Sigma_i$. The symmetrization makes $\hat{k}(\mathbf{s})$ even, $\hat{k}(\mathbf{s}) = \hat{k}(-\mathbf{s})$ for all \mathbf{s} . So the Fourier transform of \hat{k} , that is our kernel, is real, since the Fourier transform of a real even function is real. Furthermore k is symmetric, since the Fourier transform of an even function is even (cf. e.g. [17]). By expanding equation (4) we get

$$k_{\text{SM}}(\tau) = \sum_{i=1}^Q w_i k_{\text{SM},i}(\tau) \quad (5)$$

$$k_{\text{SM},i}(\tau) = \cos(2\pi \tau^\top \boldsymbol{\mu}_i) \prod_{p=1}^P \exp\left(-2\pi^2 \tau^2 \Sigma_i^{(p)}\right) \quad (6)$$

where Q is the number of components, $k_{\text{SM},i}$ is the i -th component, P is the dimension of input, $w_i, \mu_i = [\mu_i^{(1)}, \dots, \mu_i^{(P)}]$, and $\Sigma_i = \text{diag}([\sigma_i^{(1)}, \dots, \sigma_i^{(P)}])$ are weight, mean, and variance of the i -th component in the frequency domain, respectively. The inverse means $1/\mu_i$ are the i -th component periods, and the inverse standard deviations $1/\sqrt{\Sigma_i}$ are length scales, determining how quickly a component varies with the inputs. So the variance $(\sigma_i^{(P)})^2$ can be thought of as an inverse length-scale, $\mu_i^{(P)}$ as a frequency. The weights w_i specify the relative contribution of each mixture component.

5 Skewed Laplace Spectral Mixture kernel

Any stationary covariance kernel can be approximated to arbitrary precision by an SM kernel, given enough mixture components in the spectral representation, because mixtures of Gaussians are dense in the set of all distribution function [18]. However, using a large number of components can lead to overfitting when there is not enough training data. Therefore, it makes sense to introduce and study new stationary kernels. Here we propose to overcome the limitations of the SM and LKP kernels described in the Introduction by using a Skewed Laplace (SL) distribution, which can better capture skewness of peaks of the spectral density and its heavy tail characteristic. We consider the three-parameter family of skewed Laplace distributions introduced in [19], with the density

$$\varphi(s; \mu, \gamma, \sigma) = \frac{\sqrt{2}}{\sigma} \frac{\kappa}{1 + \kappa^2} \begin{cases} \exp\left(-\frac{\sqrt{2}}{\sigma\kappa}(\mu - s)\right) & \text{if } s < \mu \\ \exp\left(-\frac{\sqrt{2}\kappa}{\sigma}(s - \mu)\right) & \text{if } s \geq \mu \end{cases} \quad (7)$$

where $\kappa = \sqrt{2}\sigma/(\gamma + \sqrt{2\sigma^2 + \gamma^2})$, γ is the skewness parameter and μ and σ^2 are the mean and variance of the distribution. We then proceed to construct a real kernel from a spectral density as done for the SM kernel: symmetrize the spectral density and then apply the inverse Fourier transform to the resulting even real function. The symmetrized spectral density function for the i -th component of the SL distribution is

$$\hat{k}_{\text{SLSM},i}(s) = \frac{1}{2} (\varphi(s; \mu_i, \gamma_i, \sigma_i) + \varphi(-s; \mu_i, \gamma_i, \sigma_i)) \quad (8)$$

Note that this transformation does not destroy the skewness of the mixture components (peaks) of the spectral density: although the spectral density is symmetric around zero by construction, its peaks are skewed around their means. The inverse Fourier transform of the SL spectral density is [20]

$$\mathcal{F}_{s \rightarrow \tau}^{-1}[\varphi(s; \mu, \gamma, \sigma)](\tau) = \frac{1 + \sigma^2\tau^2/2 + \gamma\tau}{(1 + \sigma^2\tau^2/2)^2 + \gamma^2\tau^2} e^{j\mu\tau} \quad (9)$$

By Bochner's theorem [15] we obtain the Skewed Laplace Mixture kernel (SLSM kernel) as the inverse Fourier Transform of \hat{k}_{SLSM} :

$$k_{\text{SLSM}}(\tau) = \mathcal{F}_{s \rightarrow \tau}^{-1} \left[\sum_{i=1}^Q w_i \hat{k}_{\text{SLSM},i} \right](\tau). \quad (10)$$

The inverse Fourier transform of $\hat{k}_{\text{SLSM},i}$ yields the i -th component of the SLSM kernel, obtained by applying (5) to both $\varphi(s; \mu_i, \gamma_i, \sigma_i)$ and $\varphi(-s; \mu_i, \gamma_i, \sigma_i)$ and adding the resulting functions:

$$k_{\text{SLSM},i}(\tau) = \frac{C_i(\tau) \cos(\mu_i\tau) - \gamma_i\tau \sin(\mu_i\tau)}{C_i^2(\tau) + \gamma_i^2\tau^2} \quad (11)$$

where $C_i(\tau) = 1 + \frac{1}{2}\sigma_i^2\tau^2$ is an inverse Cauchy function (the inverse Fourier transform of the zero positioned non-skewed Laplace) [7]. From Equation (11) we can obtain the Skewed Laplace Mixture kernel (SLSM kernel) with Q components, corresponding to a mixture of Q SL distributions in the frequency domain,

$$k_{\text{SLSM}}(\tau) = \sum_{i=1}^Q w_i \frac{C_i(\tau) \cos(\mu_i\tau) - \gamma_i\tau \sin(\mu_i\tau)}{C_i^2(\tau) + \gamma_i^2\tau^2}. \quad (12)$$

Note that $k_{\text{SLSM},i}(\tau)$ is positive semi-definite because its corresponding spectral density is non-negative everywhere (see (8)) [15, 16] and the kernel is real valued because its spectral density is even [1]. The denominator of $k_{\text{SLSM},i}(\tau)$ is a skew function of the inverse distance and the numerator term is a periodical trigonometry function. Observe that the Cauchy function has slower decay over the distance τ than the exponential function used in SM based kernels.

5.1 SLSM extensions

The multivariate Skewed Laplace distribution is a natural extension of univariate one, and was introduced in [21, 19, 22]. This allows us to directly extend our SLSM kernel to the multivariate setting as follow:

$$k_{\text{SLSM}}(\boldsymbol{\tau}) = \sum_{i=1}^Q w_i \frac{C_i(\boldsymbol{\tau}) \cos(\boldsymbol{\tau}^\top \boldsymbol{\mu}_i) - (\boldsymbol{\tau}^\top \boldsymbol{\gamma}_i) \sin(\boldsymbol{\tau}^\top \boldsymbol{\mu}_i)}{C_i^2(\boldsymbol{\tau}) + (\boldsymbol{\tau}^\top \boldsymbol{\gamma}_i)^2}, \quad (13)$$

with C_i generalized to $C_i(\boldsymbol{\tau}) = 1 + \frac{1}{2} \boldsymbol{\tau}^\top \Sigma_i \boldsymbol{\tau}$.

5.2 Comparison with other kernels

Figure 2 provides a visual comparison of the SM, LKP and SLSM distributions used for fitting the empirical spectral density. The differences among SLSM, LKP and SM are illustrated in terms of covariance, spectral density, and sampling functions. The subplots in the second row of Figure 2 show random functions drawn from a GP with SM, LKP, and SLSM kernel, respectively. The sampled function values were obtained using 500 equally-spaced discrete points.

The inverse FT of the SM spectral density is an exponential function, so in the time domain we have an exponential decay of covariance. When we use LKP to fit the empirical spectral density and apply the inverse FT we get a Cauchy function, which decays in a much slower way than the exponential one. Using SLSM we extend the tails of the Laplace distribution (by means of the γ term in equation 7), which in the time domain yields a further reduction of the decay rate of the covariance. This phenomenon is illustrated in Figure 2, which shows longer range covariance of SLSM (middle and bottom right plots). The main characteristics of SM, LKP and SLSM can be summarized as follow:

- SM: multivariate Gaussian, dense, non-skewed peaks, short-tailed, smooth, symmetry of each peak, exponential decay of covariance;
- LKP: univariate Laplacian, sparse, non-skewed peaks, heavy-tailed, non-smooth, symmetry of each peak, fast decay of covariance;
- SLSM: multivariate skewed Laplacians, skewed peaks, one side more heavily-tailed, non-smooth, slower decay of covariance.

Figure 1 shows SLSM provides a better fit of the empirical spectral density than SM and LKP. SLSM extends the LKP kernel, which can be obtained by removing the skewness term, i.e., by setting $\gamma_i = 0$. There is also a relation between the SLSM and the Rational Quadratic (RQ) kernel,

$$k_{\text{RQ}}(\tau) = \theta_f \left(1 + \frac{\tau^2}{2\alpha\ell^2} \right)^{-\alpha} \quad (14)$$

The RQ kernel can be viewed as a scale mixture (an infinite sum) of squared scale mixture SE kernels with different characteristic length-scales [2]. The RQ kernel is considered the most general representation defining a valid isotropic covariance function in \mathbb{R}^P [16, 4]. From Equations (11) and (14) it follows that a non-skewed SLSM component $k_{\text{SLSM},i}(\tau)$ is the product of a RQ kernel with $\alpha = 1$, $\theta_f = w_i$, $\ell^{-2} = \sigma_i^2$ and a cosine kernel. Thus the RQ kernel with $\alpha = 1$ can be viewed as modeling the spectral density as one Laplace distribution at zero mean position in the frequency domain. Therefore the RQ kernel can be view as part of a component of a SLSM kernel.

SLSM components could be approximated at arbitrary precision with a mixture of Gaussians using sufficiently many components. So a SM kernel can approximate the SLSM kernel. However, as observed e.g. by [23], although mixtures of Gaussian distributions can be used to approximate any distribution, a large number of spectral mixture components might be required to account for the lower degrees of smoothness evidenced in the data. This would result in more expensive inference, and be less robust to local optima. In addition, in Figure 2 we show a comparison of SM, LKP, and SLSM with 3 components in terms of spectral densities, covariance, and sampling paths.

5.3 Hyper-parameter initialization

Kernels hyper-parameters are inferred by optimizing the negative log marginal likelihood (NLML), which is a non-convex problem for kernels such as SM and SLSM. The initialization of these hyper-parameters has a direct impact on the ability of the optimization process to find a good local optimum of the NLML. In general, SM-based kernels are particularly sensitive to the initialization of their hyper-parameters, and the SLSM kernel shares this initialization problem. Here we apply an initialization strategy which has been shown to be effective in previous works [3, 24]. These works suggest that non-smooth peaks of the empirical spectral densities are near the true frequencies and use a Gaussian

Mixture Model to fit the empirical spectral density, which is then used to initialize the hyper-parameters of an SM kernel. We make use of this result for the SLSM kernel, and initialize the hyper-parameters using a Laplace Mixture Model,

$$p_{\text{LMM}}(\Theta|\mathbf{s}) = \sum_{i=1}^Q \tilde{w}_i \varphi(\tilde{\mu}_i, \tilde{\Sigma}_i) \quad (15)$$

to fit the empirical spectral density in order to get Q cluster centers, where Q is the number of components. We use the Expectation Maximization algorithm [25] to estimate the parameters of this mixture model. The resulting estimates \tilde{w}_i , $\tilde{\mu}_i$, and $\tilde{\Sigma}_i$ are used as initial hyper-parameters values of SLSM and LKP kernels. The skewness parameter γ_i is initialized randomly between -1 and 1. We use the above initialization strategies in all our experiments on real-world datasets.

6 Experiments

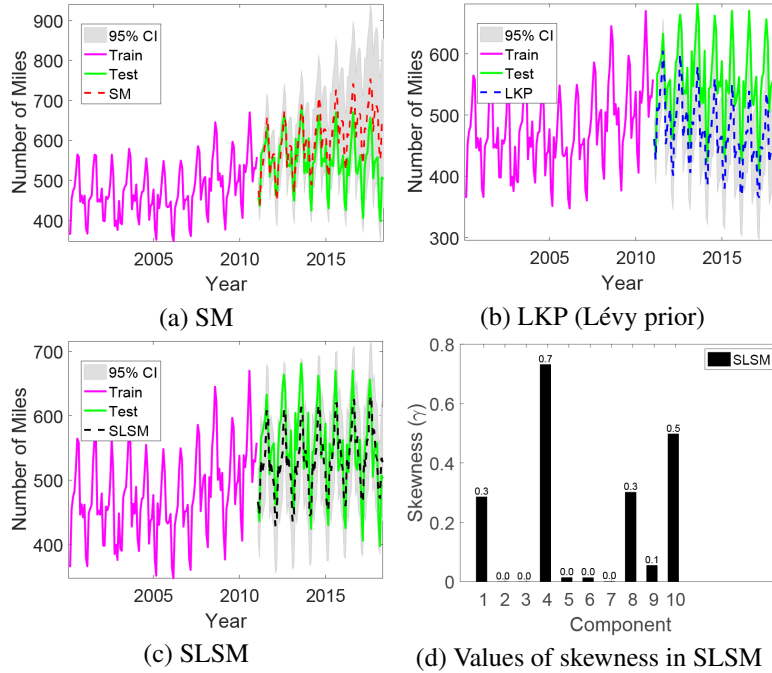


Figure 3: Extrapolation results on the Rail Passenger Miles dataset and learned skewness in SLSM. Note that the better fitting of SM and LKP on the empirical spectral densities (training data) may lead to overfitting and negatively affect extrapolation performance.

We assess the performance of SLSM and of the following popular stationary kernels available in the GPML toolbox [2, 1]: linear with bias (LIN), squared exponential (SE), piecewise polynomial (Poly), periodic (PER), rational quadratic (RQ), Matérn 5/2 (MA), Gabor, neural network (NN), additive kernel based on SE using unary and pairwise interactions (ADD); as well as SM and LKP kernels. Also, we assess the performance of the LKP kernel as an instance of SLSM with $\gamma = 0$, we denote this variant by SLSM($\gamma = 0$).

For SM we initialize the hyper-parameters using a Gaussian Mixture Model $p_{\text{GMM}}(\Theta|\mathbf{s}) = \sum_{i=1}^Q \tilde{w}_i \mathcal{N}(\tilde{\mu}_i, \tilde{\Sigma}_i)$. For LKP we use a Laplace Mixture Model. All other kernels in our comparison use the standard initialization in GPML toolbox. For LKP a Lévy process prior and reversible jump MCMC (RJ-MCMC) were considered to prune extraneous components and infer the posterior distribution, respectively, as described in [7]. For all other kernels we use exact inference together with LBFGS for optimizing the kernel hyperparameters. In all experiments we use the mean squared error (MSE) $\text{MSE} = \frac{1}{n} \sum_{i=1}^n (y_i - \tilde{y}_i)^2$, NLML, and their standard deviation as performance metrics, where \tilde{y}_i denotes the predicted value. We run each experiment for 10 times and report the standard deviation of the results.

Also, spectral density, specific skewness values, instance of skewed component, and experiments with varying values of Q in SLSM, LKP, SM are considered to provide a deeper insight on their performance. We consider forecasting tasks with real-world datasets [26]: rail miles, monthly electricity, mean sunspot, and computer hardware.

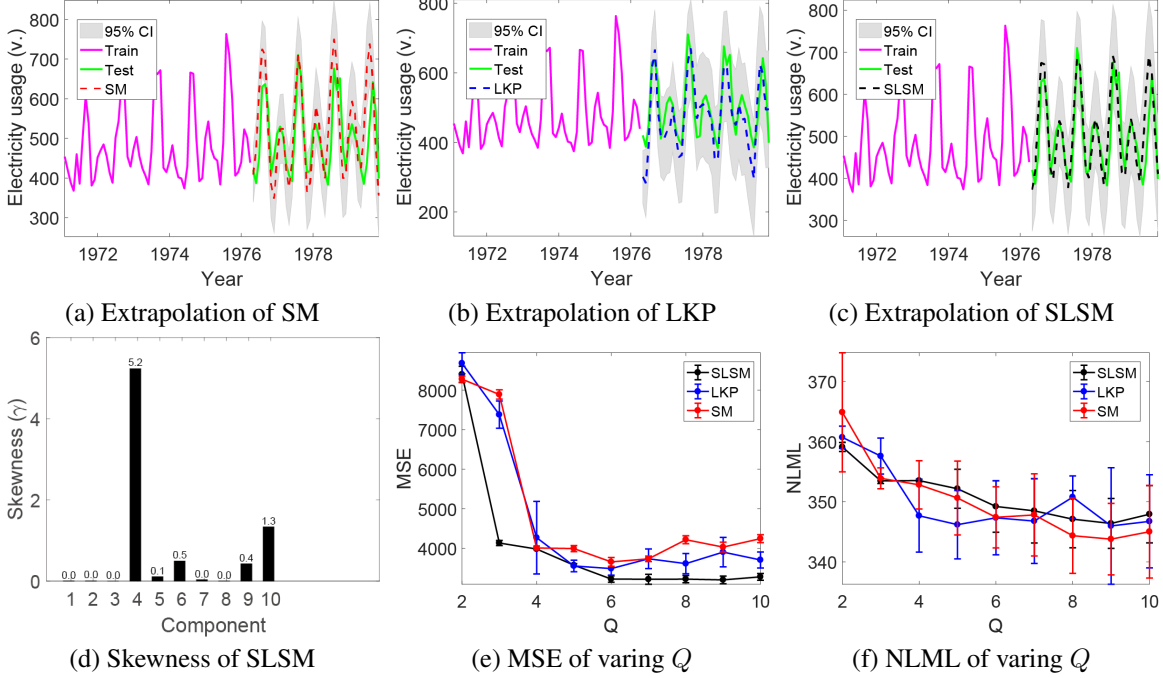


Figure 4: Extrapolation using the SM kernel (a), LKP kernel using Lévy prior (b), and SLSM kernel (c) on the monthly electricity usage dataset. The solid magenta line shows the training data, while the dashed line is the mean prediction by a GP. Plots (d), (e) and (f) show the skewness of the optimized SLSM kernels, together with MSE and NLML of varying Q . All plots for the other experiments use the same notation.

6.1 Long-term forecasting of rail passenger miles

In this experiment, we illustrate on a real-life long-term forecasting problem the differences between SM, LKP and SLSM kernels in terms of their spectral densities. We consider the rail miles dataset¹. This dataset consists of 220 values covering the period from Jan. 2000 to Apr. 2018. We use $Q = 10$ components for the SM, LKP and SLSM kernels. The top plots in Figure 3 show extrapolation results. For test points far from the last (training) observation, the SLSM kernel achieves best extrapolation performance. The bottom part of Figure 3 shows that the spectral density of the SLSM kernel has components with a higher variance than that of the other kernels as well as components with higher mean. As a result, the optimized SLSM kernel looks different from the empirical spectral density. We believe that this is the result of the extra flexibility that skewness provides, which allows the optimizer to find a better local optimum for the kernel hyperparameters. Which in turn leads to better generalization, since it can capture patterns not present in the empirical spectral density.

In contrast, the SM and LKP kernels stay closer to the empirical spectral density. Looking in more detail, we can see that the optimized SLSM kernel has components with a large mean, $\mu_5 = 1.57$, which corresponds to a smaller period of about half a month, in line with half monthly variations that appear in the dataset. In SM and LKP, their spectral density miss many of variations at higher frequencies. The specific values of weights w , means μ , variances σ^2 , and skewness γ in SLSM determine the contribution, periodicity, length-scale, and long range dependency of each SLSM component, respectively.

Overall, the SLSM kernel shows state-of-the-art performance in terms of MSE (see Table 1), while its NLML is slightly smaller than that of SM (see Table 2). This may seem surprising. However, note that NLML is the sum of two terms (and a constant term that is ignored): a model fit and a complexity penalty term. The first term is the data fit term which is maximized when the data fits the model very well. The second term is a penalty on the complexity of the model, i.e. the smoother the better. When Optimizing NLML finds a balance between the two and this changes with the data observed.

¹<https://fred.stlouisfed.org/series/RAILPM>

6.2 Forecasting long-term electricity consumption

In this experiment we investigate comparatively the performance of SM, LKP and SLSM when varying the number of components in a small range (2-10), using the real-life problem of long range monthly electricity forecasting. This is a problem of practical relevance for electric power system planning, tariff regulation and energy trading [27]. The dataset includes monthly residential electricity usage in Iowa city from Jan. 1971 to Oct. 1979. There are a total 106 time points, of which we use the first 60% for training and the rest for testing.

For SLSM, LKP, and SM we use $Q = 10$ components. Figure 4, subplots (a), (b), (c), show that SLSM has a better extrapolation performance than SM and LKP, in particular for small peaks corresponding to the winter months. Subplot (d) shows that SLSM uses the skewness, with a component having a relatively very high skewness value. Note that the inference procedure of LKP is based on RJ-MCMC, which automatically selects components. On this data, 11 components are selected. Figure 4, subplots (e) and (f), show the performance of SLSM, SLSM with $\gamma = 0$, and SM with varying number of components. Results indicate best performance of SLSM and robustness to the number of selected components.

Results in terms of MSE and NLML are given in Tables 1 and 2, respectively. They show that SLSM kernel yields best long-term extrapolation MSE performance in this experiment and larger NLML than the SM kernel.

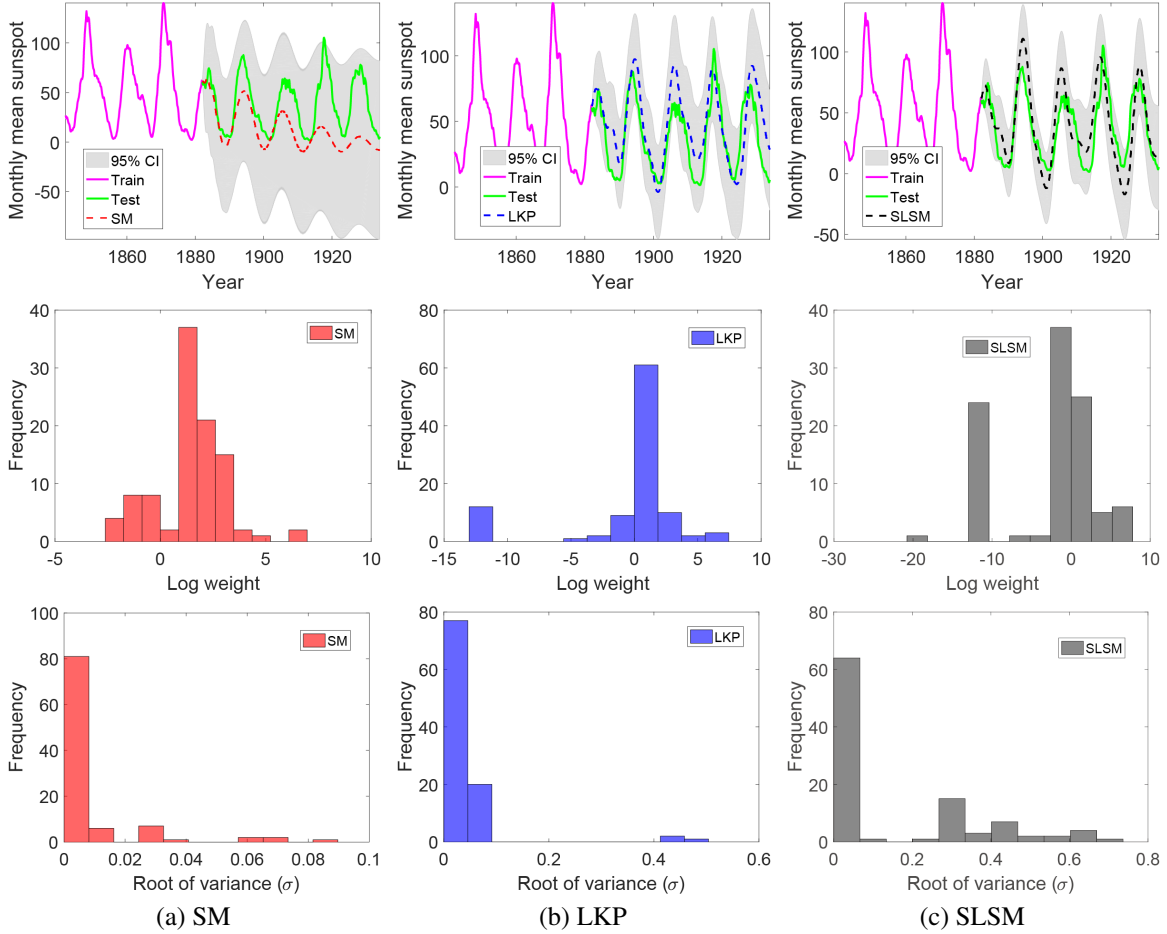


Figure 5: Extrapolation and histogram of hyper-parameters of SM, LKP, and SLSM with 100 components performed on mean sunspot dataset. First row: extrapolation of SM, LKP, SLSM. Second row: histogram of log weight $\log(w)$; Third row: histogram of variance σ ; For histogram of weights in LKP and SLSM, most of the components have very small weights close to zero, which means the LKP and SLSM are very sparse. While for SM a large number of components have weights bigger than 10, which means SM is very dense and these SM components usually have bigger magnitude in the frequency domain. On the other hand, the histogram of variance σ shows that SLSM components are much more heavy tailed with bigger variances than those of LKP and SM. SM components in the frequency domain are very short tailed, which exhibit fast decaying behaviors.

6.3 Long-term prediction of mean sunspot numbers

Here we further assess long-term forecasting capability of the considered kernels, this time with a large number of components. We consider the mean total sunspot number dataset. For this dataset the monthly number of sunspots was collected from Jan. 1842 - Dec. 1933 at the Royal Observatory of Belgium, Brussels, resulting in 1104 time points. We consider the 13-month smoothed data². We consider $Q = 100$ for the SM, LKP and SLSM kernels. In order to increase the difficulty of extrapolation and perform longer-term forecasting, we use less training samples (45%) than testing samples (55%).

Results are shown in Figure 5. In that figure we also show the hyper-parameters histogram of SM, LKP, and SLSM kernels, which indicates that in addition to long range covariance, skewness is also beneficial for robust learning in the presence of large number of components. Unlike SM and LKP, SLSM is less sensitive to the value of Q and does not need to prune the number of components in order to avoid overfitting. However a large value of Q affects the optimization time due to the larger of hyper-parameter space.

Table 1 shows improved MSE results of SLSM over the other kernels, while also in this experiment NLML of SLSM is not the smallest (see Table 2).

6.4 Long-term forecasting with multivariate time series data

We now investigate the performance of the considered spectral kernels on a long-term extrapolation task with multivariate data. We consider a multidimensional computer hardware dataset. The dataset recorded relative CPU performance collected on Oct. 1987. There are 209 multivariate instances and the following 8 input variables: vendor name, model name, machine cycle time, minimum main memory, maximum main memory, cache memory, minimum channels, maximum channels. The task is to predict CPU relative performance. Also in this experiment we use $Q = 10$ components for SLSM and SM.

LKP with Lévy prior and MCMC inference was developed and tested on one-dimensional data. So, in order to compare LKP with SLSM we consider our multidimensional version of LKP obtained by means of SLSM with $\gamma = 0$ with standard exact inference instead of MCMC-RJ. The other baseline kernels use automatic relevance determination (ARD) to scale each dimension independently. Results of this experiment, in terms of MSE and NLML are given in Table 1 and Table 2, respectively.

Table 1: Performance comparisons between SLSM and other kernels in terms of MSE.

Kernel	Rail miles	Electricity	Sunspot	Computer
LIN	6910.03 \pm 870.64	9796.69 \pm 498.52	4412.69 \pm 1296.47	1850.49 \pm 48.96
SE	206248.45 \pm 98312.03	251271.77 \pm 3599.75	2124.62 \pm 70.78	36156.20 \pm 4739.64
Poly	304891.58 \pm 4891.04	260211.15 \pm 1831.73	2178.87 \pm 139.67	41472.44 \pm 2529.99
PER	9107.06 \pm 581.37	10787.98 \pm 5386.39	2265.81 \pm 1152.55	25265.85 \pm 816.35
RQ	8432.82 \pm 2541.86	11495.00 \pm 1688.50	2174.84 \pm 115.45	5401.76 \pm 1173.73
MA	259732.10 \pm 20191.90	238184.59 \pm 7416.91	2258.18 \pm 221.42	34239.31 \pm 5513.41
Gabor	304876.73 \pm 4883.92	260534.61 \pm 2019.31	2236.29 \pm 148.05	42641.77 \pm 224.18
NN	5158.80 \pm 332.93	9652.25 \pm 1783.46	1234.07 \pm 107.75	12238.99 \pm 1146.74
ADD	282872.89 \pm 15384.09	250703.87 \pm 3324.76	2265.31 \pm 178.22	676.42 \pm 85.40
SM	4526.84 \pm 571.47	4792.03 \pm 371.95	1241.99 \pm 261.32	559.24 \pm 52.46
LKP	5023.39 \pm 580.60	4256.87 \pm 423.73	613.26 \pm 74.18	— \pm —
SLSM ($\gamma = 0$)	4225.38 \pm 568.97	3476.00 \pm 197.33	384.66 \pm 32.21	538.04 \pm 42.05
SLSM	1465.53 \pm 220.37	3181.92 \pm 116.46	313.59 \pm 22.39	297.89 \pm 25.59

6.5 Discussion

Overall the experiments a GP with the SLSM kernel has consistently lower MSE than the other kernel, but its NLML is not always the lowest. A reason for this phenomenon could be that the marginal likelihood surfaces for the GPs of SM, LKP, and SLSM usually have many local optima. A lower NLML values corresponding to a local optimum perhaps is caused by overfitting, which leads to poor generalization performance to extrapolate unseen points.

We can see that compared to other kernels, the spectral density of the SLSM kernel tends to have very sharp peaks, that is, components with a low variance. Since the variance in the frequency domain is inversely related to the variance in the time domain, these components will lead to a kernel with long-range covariances in the time domain. This can explain the good extrapolation performance of the kernel. Moreover, compared to the SM and LKP kernels, the SLSM kernel can discover more short period patterns, corresponding to spectral density components with large means. In

²<http://www.sidc.be/silso/datafiles>

Table 2: Comparisons of negative log likelihood between SLSM and other kernels.

Kernel	Rail miles	Electricity	Sunspot	Computer
LIN	694.28 ± 100.97	321.00 ± 70.27	1336.73 ± 380.11	625.80 ± 14.54
SE	671.65 ± 151.09	339.28 ± 49.54	1784.03 ± 540.17	548.40 ± 94.32
Poly	935.16 ± 135.22	379.36 ± 67.00	2620.25 ± 546.63	622.49 ± 114.72
PER	715.60 ± 64.43	359.57 ± 96.20	1702.36 ± 279.06	745.53 ± 3.43
RQ	663.92 ± 96.42	338.61 ± 46.01	1639.60 ± 576.88	257.58 ± 50.85
MA	770.05 ± 78.73	339.52 ± 77.41	1898.71 ± 715.64	583.53 ± 61.66
Gabor	936.73 ± 136.08	415.28 ± 79.01	2258.31 ± 603.26	824.79 ± 23.99
NN	744.31 ± 13.21	358.92 ± 57.99	1043.50 ± 171.84	420.22 ± 17.38
ADD	765.99 ± 22.14	335.57 ± 68.51	791.92 ± 223.85	302.99 ± 4.51
SM	595.68 ± 11.78	263.68 ± 29.40	712.76 ± 112.35	180.21 ± 11.93
LKP	699.34 ± 21.29	334.31 ± 5.00	612.06 ± 4.64	— ± —
SLSM ($\gamma = 0$)	686.14 ± 23.04	339.51 ± 3.45	612.01 ± 2.95	217.05 ± 5.16
SLSM	658.63 ± 14.54	246.61 ± 8.97	611.43 ± 1.94	205.29 ± 5.23

general the long-term variation is more important for extrapolation because short period patterns mixed with noise and specific local factors are difficult to capture. In this paper, we performed SLSM, LKP, SM with $Q = 10$, Q between 2 and 10 and $Q = 100$. In all these settings, SLSM achieved state of the art extrapolation results.

7 Conclusion

We proposed a new kernel for long-term forecasting, derived in a principled way by modeling the empirical spectral densities using a skewed Laplace spectral mixture (SLSM) whose characteristics are more in agreement with those of the DFT distribution than e.g. the Gaussian mixture used in SM kernels. The corresponding SLSM kernel has empirically been shown to achieve state-of-the-art performance on long-term forecasting tasks and extrapolation of missing parts of a signal.

The SLSM kernel also has a connection with RQ kernel, which not only provides a new interpretation of the RQ kernel, but also demonstrates the usefulness of the SLSM kernel as a principled alternative to the exponential and RQ kernels. We might further extend SLSM to increase its long-range modeling capability by using a RQ kernel with $\alpha < 1$ instead of the Cauchy function term of the SLSM kernel. Experiments on four real-world datasets have demonstrated that by using the SLSM kernel dense structures as well as sparse structures in the data can be captured. In addition, the SLSM kernel was shown to be able to learn more periodical patterns, particularly short-term patterns in the data.

The SLSM kernel can also be generalized to Cartesian structured multidimensional datasets like images following [28, 4, 11, 29]. The multidimensional SLSM kernel becomes:

$$k_{\text{SLSM}}(\tau) = \prod_{p=1}^P \sum_{i=1}^Q k_{\text{SLSM},i}^{(p)}(\tau) \quad (16)$$

where $k_{\text{SLSM},i}^{(p)}(\tau)$ is the i -th SLSM component on the p -th dimension. Equation (16) can be used for fast inference by decomposing K_{SLSM} as the Kronecker product of matrices over each input dimension $K_{\text{SLSM}} = K_{\text{SLSM}}^1 \otimes \dots \otimes K_{\text{SLSM}}^P$. It is interesting to investigate applications involving such data. Other future interesting research involves non-stationary, compositional, and multi-task extensions of the SLSM kernel.

Acknowledgment

The work was supported by the Radboud University.

References

- [1] Carl Edward Rasmussen and Hannes Nickisch. Gaussian processes for machine learning (gpml) toolbox. *Journal of Machine Learning Research*, 11(Nov):3011–3015, 2010.
- [2] Carl Edward Rasmussen and Christopher KI Williams. *Gaussian process for machine learning*. MIT press, 2006.
- [3] Andrew Wilson and Ryan Adams. Gaussian process kernels for pattern discovery and extrapolation. In *Proceedings of the 30th International Conference on Machine Learning (ICML-13)*, pages 1067–1075, 2013.

- [4] Andrew Gordon Wilson. Covariance kernels for fast automatic pattern discovery and extrapolation with Gaussian processes. *University of Cambridge*, 2014.
- [5] David Duvenaud, James Robert Lloyd, Roger Grosse, Joshua B Tenenbaum, and Zoubin Ghahramani. Structure discovery in nonparametric regression through compositional kernel search. *arXiv preprint arXiv:1302.4922*, 2013.
- [6] Sami Remes, Markus Heinonen, and Samuel Kaski. Non-stationary spectral kernels. In *Advances in Neural Information Processing Systems*, pages 4645–4654, 2017.
- [7] Phillip A Jang, Andrew Loeb, Matthew Davidow, and Andrew G Wilson. Scalable Levy process priors for spectral kernel learning. In *Advances in Neural Information Processing Systems*, pages 3943–3952, 2017.
- [8] S. Gazor and Wei Zhang. Speech probability distribution. *Signal Processing Letters IEEE*, 10(7):204–207, July 2003.
- [9] Torbjørn Eltoft, Taesu Kim, and Te-Won Lee. On the multivariate Laplace distribution. *IEEE Signal Process. Lett.*, 13(5):300–303, 2006.
- [10] Julià Minguillón and Jaume Pujol. JPEG standard uniform quantization error modeling with applications to sequential and progressive operation modes. *J. Electronic Imaging*, 10(2):475–485, 2001.
- [11] Andrew G Wilson, Elad Gilboa, Arye Nehorai, and John P Cunningham. Fast kernel learning for multidimensional pattern extrapolation. In *Advances in Neural Information Processing Systems*, pages 3626–3634, 2014.
- [12] Seth Flaxman, Andrew Wilson, Daniel Neill, Hannes Nickisch, and Alex Smola. Fast kronecker inference in Gaussian processes with non-Gaussian likelihoods. In *International Conference on Machine Learning*, pages 607–616, 2015.
- [13] Junier B Oliva, Avinava Dubey, Andrew G Wilson, Barnabás Póczos, Jeff Schneider, and Eric P Xing. Bayesian nonparametric kernel-learning. In *Artificial Intelligence and Statistics*, pages 1078–1086, 2016.
- [14] Te Won Lee Hyun Jin Park. Modeling nonlinear dependencies in natural images using mixture of Laplacian distribution, 2004.
- [15] Salomon Bochner. *Lectures on Fourier Integrals.(AM-42)*, volume 42. Princeton University Press, 2016.
- [16] ML Stein. Interpolation of spatial data: some theory for kriging., 1999.
- [17] Forrest Hoffman. An introduction to fourier theory. *Extraído el*, 2, 1997.
- [18] N Kostantinos. Gaussian mixtures and their applications to signal processing. *Advanced signal processing handbook: theory and implementation for radar, sonar, and medical imaging real time systems*, pages 3–1, 2000.
- [19] Samuel Kotz, Tomaz J Kozubowski, and Krzysztof Podgórski. Asymmetric multivariate laplace distribution. In *The Laplace distribution and generalizations*, pages 239–272. Springer, 2001.
- [20] Konstantinos Fragiadakis and Simos G Meintanis. Goodness-of-fit tests for multivariate laplace distributions. *Mathematical and Computer Modelling*, 53(5-6):769–779, 2011.
- [21] Tomasz J. Kozubowski and Krzysztof Podgórski. A multivariate and asymmetric generalization of laplace distribution. *Computational Statistics*, 15(4):531–540, Dec 2000.
- [22] Helle Visk. On the parameter estimation of the asymmetric multivariate laplace distribution. *Communications in Statistics—Theory and Methods*, 38(4):461–470, 2009.
- [23] Yves-Laurent Kom Samo and Stephen Roberts. Generalized spectral kernels. *arXiv preprint arXiv:1506.02236*, 2015.
- [24] William Herlands, Andrew Wilson, Hannes Nickisch, Seth Flaxman, Daniel Neill, Wilbert Van Panhuis, and Eric Xing. Scalable Gaussian processes for characterizing multidimensional change surfaces. In *Artificial Intelligence and Statistics*, pages 1013–1021, 2016.
- [25] Tood K Moon. The expectation-maximization algorithm. *IEEE Signal Processing Magazine*, 13(6):47–60, 1997.
- [26] Rob J Hyndman and M Akram. Time series data library. Available from Internet: <http://robjhyndman.com/TSDL>, 2010.
- [27] José Francisco Moreira Pessanha and Nelson Leon. Forecasting long-term electricity demand in the residential sector. *Procedia Computer Science*, 55:529–538, 2015.
- [28] Andrew Gordon Wilson and Hannes Nickisch. Kernel interpolation for scalable structured Gaussian processes (KISS-GP). In Francis R. Bach and David M. Blei, editors, *Proceedings of the 32nd International Conference on Machine Learning, ICML 2015, Lille, France, 6-11 July 2015*, volume 37 of *JMLR Workshop and Conference Proceedings*, pages 1775–1784. JMLR.org, 2015.

- [29] Elad Gilboa, Yunus Saatci, and John P. Cunningham. Scaling multidimensional inference for structured Gaussian processes. *IEEE Trans. Pattern Anal. Mach. Intell.*, 37(2):424–436, 2015.